The microplastisphere: biodegradable microplastics addition alters soil microbial community structure and function

Zhou, Jie; Gui, Heng; Banfield, Callum; Wen, Yuan; Dippold, Michaela A.; Charlton, Adam; Jones, Davey L.

Soil Biology and Biochemistry

DOI:
10.1016/j.soilbio.2021.108211

Published: 01/05/2021

Peer reviewed version

The microplastisphere: biodegradable microplastics addition alters soil microbial community structure and function

Jie Zhou[a,b†], Heng Gui[c,d†], Callum C. Banfield[b], Yuan Wen[a], Huadong Zang[a,*], Michaela A. Dippold[b], Adam Charlton[e], Davey L. Jones[f,g]

[a] *College of Agronomy and Biotechnology, China Agricultural University, Beijing, China*

[b] *Biogeochemistry of Agroecosystems, Department of Crop Sciences, University of Goettingen, Goettingen, Germany*

[c] CAS *Key Laboratory for Plant Diversity and Biogeography of East Asia, Kunming Institute of Botany, Chinese Academy of Science, Kunming, China*

[d] *Centre for Mountain Futures (CMF), Kunming Institute of Botany, Chinese Academy of Science, Kunming, Yunnan, China*

[e] *BioComposites Centre, Bangor University, Bangor, Gwynedd, LL57 2UW, UK*

[f] *School of Natural Sciences, Bangor University, Bangor, Gwynedd, LL57 2UW, UK*

[g] *Soils West, UWA School of Agriculture and Environment, The University of Western Australia, Crawley, WA 6009, Australia*

*Corresponding author

E-mail address: zanghuadong@cau.edu.cn

†These authors contributed equally to this study

Graphical abstract

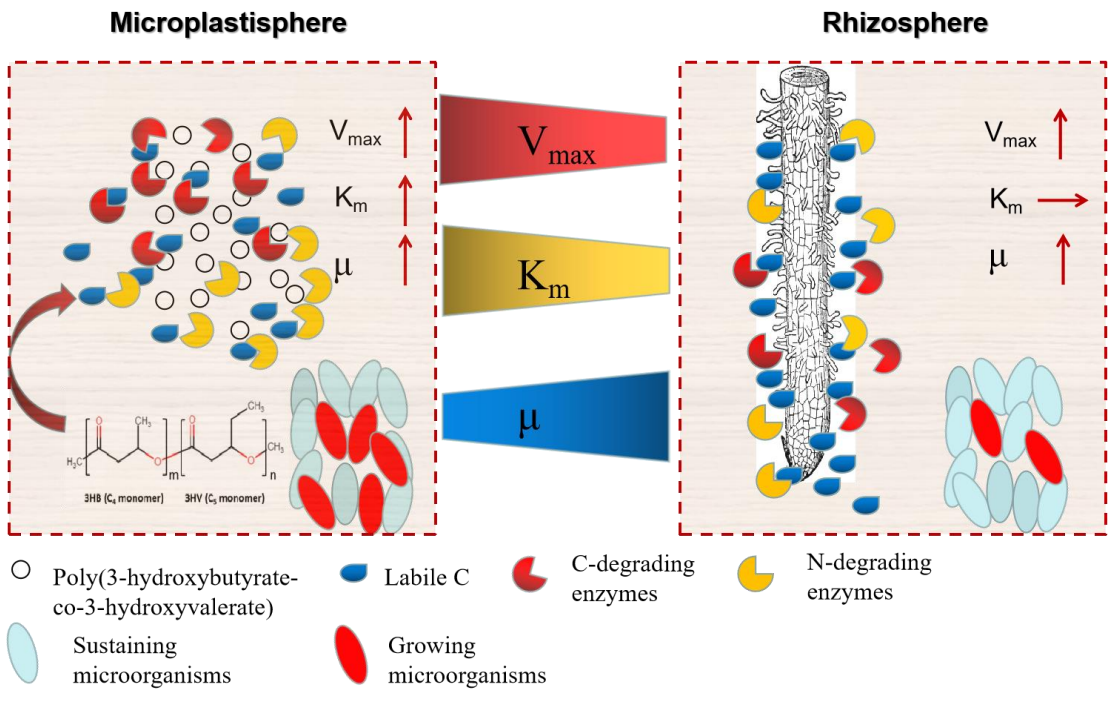

Abstract

Plastic accumulating in the environment, especially microplastics (defined as particles <5 mm), can lead to a range of problems and potential loss of ecosystem services. Polyhydroxyalkanoates (PHAs) are biodegradable plastics used in the manufacture of mulch films, and packaging as an alternative to minimize plastic residue accumulation and reduce soil pollution. Little is known, however, about the effect of microbioplastics on soil-plant interactions, especially soil microbial community structure and functioning in agroecosystems. For the first time, we combined zymography (to localize enzyme activity hotspots) with substrate-induced growth respiration to investigate the effect of PHA addition on soil microbial community structure, growth, and exoenzyme kinetics in the microplastisphere (i.e. interface between soil and microplastic particles) compared to the rhizosphere and bulk soil. We used the common PHA biopolymer, poly (3-hydroxybutyrate-*co*-3-hydroxyvalerate) (PHBV) to show that PHBV was readily used by the microbial community as a source of carbon (C) resulting in an increased specific microbial growth rate and a more active microbial biomass in the microplastisphere in comparison to the bulk soil. Higher β-glucosidase and leucine aminopeptidase activities (0.6-5.0 times higher V_{max}) and lower enzyme affinities (1.5-2.0 times higher K_m) were also detected in the microplastisphere relative to the rhizosphere. Furthermore, the PHBV addition changed the soil bacterial community at different taxonomical levels and increased the alpha diversity, as well as the relative abundance of *Acidobacteria* and *Verrucomicrobia* phyla, compared to the untreated soils. Overall, PHBV addition created soil hotspots where C and nutrient turnover is greatly enhanced, mainly driven by the accelerated microbial biomass and activity. In conclusion, microbioplastics have the potential to alter soil ecological functioning and

biogeochemical cycling (e.g., SOM decomposition).

Keywords: enzyme activity; microbial growth; microplastic pollution; soil organic matter

1. Introduction

Synthetic polymers are widely used in our daily lives (Wright and Kelly, 2017), and more than 280 million tons of plastics are produced annually (Duis and Coors, 2016; Sintim and Flury, 2017). Despite the remarkable benefit of plastics to society, there are increasing concerns associated with the vast amount of plastic entering our environment and its subsequent resistance to degradation (Rochman, 2018). These concerns are supported by estimates that > 30% of the world's plastic waste is disposed of inappropriately, with most ultimately entering the soil ecosystem (Jambeck et al., 2015; Weithmann et al., 2018). In soils, larger plastic debris often becomes fragmented by biota and physical disturbance into smaller pieces known as microplastics (mean diameter < 5 mm), which have received increased attention globally, due to their potential to cause environmental damage (Rillig, 2012; Wright and Kelly, 2017; de Souza Machado et al., 2019). A promising approach to overcome the accumulation of microplastics in soils is to replace traditional petroleum-based plastics with biodegradable bioplastics like polyhydroxyalkanoates (PHAs; Gross and Kalra, 2002; Volova et al., 2017). PHAs account for 5.6% of the global production capacity for biodegradable polymers, and represent the second fastest growing group in the market sector since 2014 (Haider et al., 2019). Even though PHAs are used in an attempt to decrease microplastic residues in terrestrial ecosystems, and praised as promising alternatives for a diverse range of applications (e.g., mulch films for agriculture), the potential environmental consequences of PHAs have not yet been thoroughly studied.

Unlike petroleum-based microplastics, which biodegrade extremely slowly, PHAs can be broken down by a range of organisms and are not thought to produce any harmful by-products (Volova et al., 2017; Haider et al., 2019; Sander et al., 2019).

Their biological source also means that they are viewed as C neutral (Garrison et al., 2016), although this assumes that they don't induce positive priming of soil organic matter (SOM). Furthermore, they are supposed to not enhance N_2O and CH_4 release which might offset these benefits. Given that PHAs are C-rich but nutrient-poor (i.e. no N and P; Gross and Kalra, 2002; Volova et al., 2017), they may alter microbial community composition and functioning during degradation. Since the decomposition of C-rich residues is associated with N and P immobilization, subsequent plant growth may also be affected due to the increased competition between plants and soil microorganisms for nutrients (Qi et al., 2018; Qi et al., 2020b; Song et al., 2020; Zang et al., 2020). In response to the additional C supplied from PHAs breakdown, the turnover of native SOM may be stimulated due to the altered metabolic status of the microbial community (Kuzyakov, 2010; Zang et al., 2017), and thus influence soil C and nutrient cycling. PHAs are also naturally present in soil being produced as storage compounds by the bacterial community (Mason-Jones et. al. 2019). Given that bacteria are more sensitive to environmental changes (e.g. increased labile C) compared to fungi (Barnard et al., 2012), soil bacteria may have a stronger response due to the increased C availability through PHAs breakdown. This will lead to significant long-term impacts on a range of soil ecosystem services (e.g., C storage, nutrient cycling, and pollutant attenuation; Zang et al., 2018). Although recent studies revealed that microplastics may have divergent influences on soil microbial communities and enzyme activities, e.g., activation (Liu et al., 2017; de Souza Machado et al., 2019), suppression (Fei et al., 2020), or remaining unchanged (Zang et al., 2020), the effect of microbioplastics on soil microorganisms remain poorly understood. Therefore, it is vital to investigate how biodegradable microplastics affect microbial functions and below-ground C processes (Zang et al., 2019, 2020; Qi et al.,

2020a).

Similar to plant-soil interactions in the rhizosphere, the main processes affected by microplastic input may occur at the soil-plastic interface (here defined as the microplastisphere). We hypothesize that these interactions are stimulated by the input of labile C present in microbioplastics (i.e. increased microbial activity, attract or favor specific bacterial taxa, and interfere with belowground plant-microorganisms interactions) leading to the formation of microbial hotspots in soil, similar to those seen in the rhizosphere (Kuzyakov and Blagodatskaya, 2015; Zang et al., 2016; Zhou et al., 2020b). Following PHAs addition, we predict that changes in soil physico-chemical properties will only occur close to the microplastic particles, with changes in the bulk soil (non-hotspot) likely to be minor (Zettler et al., 2013; Huang et al., 2019). The specific niches of the microorganisms in the microplastisphere are of ecological relevance, given that most agricultural soils are contaminated by microplastics (Steinmetz et al., 2016; Qi et al., 2020a). However, it still remains unclear how PHAs affect soil microbial communities in hotspots and, thus, alters soil C and nutrient cycling.

Here, for the first time, we coupled zymography, a method to accurately locate microbial hotspots (Hoang et al., 2020; Zhang et al., 2020), the kinetics of exoenzyme activities involved in C, N, and P cycling, microbial growth, and bacterial community structure to evaluate microbial functions, as well as soil process in hotspots (rhizosphere and microplastisphere) and bulk soil. Poly (3-hydroxybutyrate-*co*-3-hydroxyvalerate) (PHBV) represents a commercially available copolymer used for mulch film production. Compared to PHB, it has higher flexibility, thermal stability, and processibility due to the monomeric composition, which makes it promising as a typical example of PHAs (Table. S1; Jiang et al., 2009;

Bugnicourt et al., 2014). Therefore, we aimed to 1) identify microbial hotspots *in situ* in soil treated with PHBV; 2) investigate the effect of biodegradable microplastics on microbial growth and enzyme kinetics; 3) evaluate changes in bacterial community structure and function in the microplastisphere and rhizosphere. We hypothesized that: 1) the labile C in PHBV will greatly alter soil bacterial community structure and functioning compared to the rhizosphere and bulk soil, and 2) the microplastisphere contains microorganisms with a high growth rate and enzyme activity in comparison to rhizosphere and bulk soil.

2. Materials and methods

2.1 Site description and sampling

Soil samples were taken from the Ap horizon (0-20 cm) of an experimental field at the Reinshof Research Station of the Georg-August University of Göttingen, Germany (28°33’26”N, 113°20’8”E). This experimental site was established more than 40 years ago and the farming history is clear. No plastic mulch was applied, and no plastic pollution was recorded for the site. The soil was air-dried, sieved (<2 mm), and mixed to achieve a high degree of homogeneity and to reduce the variability among replicates. Fine roots and visible plant residues were carefully removed prior to use. The soil contained 1.3% total C, 0.14% total N, and had a pH of 6.8 (Zhou et al., 2020b). Ten percent (w/w) of the soil dry weight was added as poly (3-hydroxybutyrate-*co*-3-hydroxyvalerate) ($[COCH_2CH(CH_3)O]m[COCH_2CH(C_2H_5)O]_n$ (PHBV). PHBV was obtained in a pelletized form from the Tianan Biologic Materials Company Ltd., Beilun, Ningbo, China. PHBV represents one of the most widespread and best characterized members of the PHA family (Bugnicourt et al., 2014). It is a 100% biobased thermoplastic

linear aliphatic (co-)polyester obtained from the copolymerization of 3-hydroxybutanoic acid and 3-hydroxypentanoic acid which are produced through the bacterial fermentation of sugars and lipids (Zinn et al., 2001). Most of the PHBV is composed of hydroxybutyrate, however, a small fraction of hydroxyvalerate is present in its polymeric backbone (Rivera-Briso and Serrano-Aroca, 2018). This type and amount of highly crystalline plastic were chosen to simulate the localized disposal of bioplastics in agricultural soils (e.g., ploughing in of mulch film residues at the end of the field season) and was based on field investigations and a review of the literature (Fuller and Gautam, 2016; Qi et al., 2020a). We added very high amounts of microplastic to reflect soil hotspots with higher contamination levels (1-20%).

2.2 Experimental design

A mesocosm experiment with a completely randomized design and four replicates was set up in a climate-controlled room. For the PHBV addition treatment, 400 g soil and PHBV were mixed homogeneously and then placed in a rhizobox (10 × 10 × 4 cm; Qiangsheng Co., Ltd. Heibei, China). The control treatment contained soil (400 g) without PHBV, but with a comparable soil disturbance. The soil bulk density was maintained at 1.2 g cm^{-3} for all rhizoboxes. Prior to use, the soil was pre-incubated under field-moist (25% v/v) conditions in a greenhouse for one week to allow the soil to equilibrate. Before planting, wheat (*Triticum aestivum* L.) seeds were sterilized in 10% H_2O_2 for 10 min, then rinsed with deionized water and germinated on wet filter paper. Five days after germination, seedlings were transplanted in rhizoboxes (one seedling per rhizobox), and then moved to the climate-controlled chamber (day/night regime of 14 h/24 °C and 10 h/14 °C, respectively). The relative humidity in the chamber was maintained at 40% and the plants were received 800

μmol m^{-2} s^{-1} photosynthetic active radiation (PAR) at canopy height (Zhou et al., 2020b). Plants were watered every three days and the soil moisture was maintained at a gravimetric moisture content of 25% throughout the experiment by weighing the rhizoboxes.

2.3 Hotspot identification

At 24 days after transplanting, zymography was used to visualize three hydrolytic enzymes Razavi et al. 2016). Given that β-glucosidase, acid phosphatase, and leucine-aminopeptidase play a corresponding major role in cellulose, organic phosphate, and protein degradation (Lopez-Hernandez et al., 1993; Lammirato et al., 2010), there reflects key enzymes related to soil C, P and N cycle, respectively (German et al., 2011). Polyamide membrane (Tao yuan, China) were saturated with 4-methylumbelliferyl (MUF) and 7-amido-4-methylcoumarin (AMC) based substrate to visualize the specific enzymes. Each substrate was separately dissolved in 10 mM MES and TRIZMA buffer for MUF and AMC, respectively. The saturated membranes were placed on soil surfaces containing root systems and covered with aluminum foil to avoid water evaporation and moisture changes during the incubation period (Hoang et al., 2020). After incubation for 1 h, the membrane were carefully lifted off the soil surface and any attached soil particles were gently removed with tweezers and a soft brush (Razavi et al., 2016). Enzyme detection sequences followed as: β-glucosidase, acid phosphatase, leucine-aminopeptidase activity, with 1 h interval after each zymography. The grey scale values transferred to the enzyme activities was calibrated using membranes (2 × 2 cm) saturated with a range of concentrations of

corresponding products, i.e. MUF and AMC (0. 0.01, 0.2, 0.5, 1, 2, 5 mM).

The zymograms were transferred into a 16-bit gray scale by ImageJ with a correction for environmental variations and camera noise (Razavi et al., 2016). The calibration line obtained for each enzyme was used to convert gray values of each zymography pixel into enzyme activities (Hoang et al., 2020). Enzyme activities exceeding 25% of mean corresponding activity of the whole soil were defined as hotspots (Zhang et al., 2020). Specifically, soil with a high color intensity (dark-red) represents microbial hotspots, whilst dark-blue colors indicate bulk soil on the zymograms (Fig. 1; Hoang et al., 2020). Given the hotspots in the control and PHBV-treated soil were detected at the distance within 1.5-2 mm from the roots and microplastics, the hotspots in the control and PHBV-treated soil were identical as the rhizosphere and microplastisphere zones, respectively (Fig. 1). After collecting soil from hotspots and bulk soil, a total of 16 samples [2 treatments (without and with PHBV)×2 microsites from each treatment (hotspots and bulk soil)×4 replicates] were obtained.

2.4 Plant and soil sampling

At 25 days after transplanting, the shoots were cut off at the base of the stem and the roots were collected separately. For precise localized sampling, soil particles were carefully collected using needles (tip 1.5 mm) directly from the hotspots (rhizosphere and microplastisphere) identified by zymography (Fig. 1). Bulk soil was collected in a similar way. Once collected, soil samples (hotspots and bulk soil) were separated into two sub-samples. One sub-sample was stored at -80 °C to analyze the bacterial

community structure, while another sub-sample was used to measure enzyme kinetics and the kinetics of substrate-induced growth respiration directly. After removal of the hotspot samples and bulk soil, the remaining soil in the rhizobox was mixed and then stored at 4 °C to measure microbial biomass N, dissolved organic C and N. Shoots and roots were oven-dried (60 °C, 5 days) and then weighed.

Soil microbial biomass N (MBN) was extracted with K_2SO_4 (32 mL, 0.05 M), and calculated with a corresponding K_{EN} factor of 0.45 according to Wen et al. (2020). Briefly, the fresh soil was homogenized and 8 g sub-sample of the soil was extracted with K_2SO_4 (32 mL, 0.05 M). Another 8 g sub-sample of the soil was fumigated with chloroform for 24 h and then extracted in the same way. Total C in extracts was measured using a 2100 TOC/TIC analyzer (Analytik Jena GmbH, Jena, Germany). The non-fumigated extractions were used as a measure for dissolved organic C (DOC) and N (DON).

2.5 Enzyme kinetics

The activity of the exoenzymes β-1,4-glucosidase (BG) (EC 2.2.1.21), leucine aminopeptidase (LAP) (EC 3.4.11.1), and acid phosphatase (ACP) (EC 3.1.3.2) were determined by the 4-methylumbelliferyl (MUF)-based and 7-amido-4-methylcoumarin (AMC)-based artificial substrates (Marx et al., 2001; Wen et al., 2019). Briefly, 0.5 g soil was mixed with 50 ml sterile water and then shaking for 30 min. After 2 min low-energy sonication (40 J s^{-1}) by ultrasonic disaggregation, 50 µl of the soil suspension, 50 µl of corresponding buffer (MES or TRIZMA) and 100 µl of the corresponding substrates at concentrations of 2, 5, 10, 20, 50, 100 and 200 µmol l^{-1} were pipetted into 96-well black microplates (Brand® plates pureGrade,

Sigma-Aldrich, Germany). The Victor 1420-050 Multi label Counter (Perkin Elmer, USA) was used to measure the fluorescence at an excitation wavelength of 355 nm and an emission wavelength of 460 nm. Enzyme activities were taken at 4 times (0, 30 min, 1 h and 2 h), and was expressed as nmol g^{-1} soil h^{-1}.

To calculate key parameters describing the enzyme kinetics, we fitted a Michaelis-Menten equation to the experimental data (Marx et al., 2001):

$$V = \frac{V_{max} \times [S]}{K_m + [S]} \quad (1)$$

where V is the enzymatically mediated rate of reaction, V_{max} is the maximal rate of reaction, K_m (Michaelis constant) is the substrate concentration at ½V_{max} and S is substrate concentration. The substrate turnover time (T_t) was calculated according to the following equation: T_t (hours) = (K_m + S) / V_{max}, where S is the substrate concentration (200 μmol l^{-1}). The catalytic efficiency of enzymes (K_a) was calculated by the ratio of V_{max} and K_m (Hoang et al., 2020). The microbial metabolic limitation was quantified by calculating the vector lengths and angles of enzymatic activity for all data based on untransformed proportional activities (e.g. (BG):(BG+LAP), (BG):(BG+ACP)) (Moorhead et al., 2016).

2.6 Kinetics of substrate-induced growth respiration

The substrate-induced growth respiration (SIGR) approach was used to distinguish total and active biomass fractions, as well as microbial specific growth rate and lag-time before growth (Zhang et al., 2020; Zhou et al., 2020a). It should be noted that although C substrate addition is required for the SIGR approach, all kinetic parameters analyzed by SIGR represent the intrinsic features of dominating microbial

populations before substrate addition (Blagodatsky et al., 2000).

One gram of fresh soil was amended with a mixture containing 10 mg g^{-1} glucose, 1.9 mg g^{-1} $(NH_4)_2SO_4$, 2.25 mg g^{-1} K_2HPO_4, and 3.8 mg g^{-1} $MgSO_4 \cdot 7H_2O$, and placed in a Rapid Automated Bacterial Impedance Technique bioanalyzer (RABIT; Microbiology International Ltd, Frederick, MD, USA), for measuring CO_2 production at room temperature (22 °C). Firstly, we pre-incubated 16 samples from hotspots and bulk soil with and without PHBV amendment for 2 days at 45% water holding capacity (WHC) to minimize the effect of sampling disturbance. To measure substrate-induced respiration, a mixture of glucose and nutrients was added and the samples were further incubated for five days at 75% WHC (Blagodatskaya et al., 2010; Zhou et al., 2020a). The evolving CO_2 was trapped in a KOH solution where the impedance of the solution was continuously measured. The average value of CO_2 emission during the 3 h before and after adding substrates were taken as basal respiration (BR), and substrate-induced growth respiration (SIGR).

Microbial respiration in glucose amended soil was used to calculate the following kinetic parameters: the microbial maximal specific growth rate (μ), the growing microbial biomass (GMB) that capable for immediate growth on glucose, the total microbial biomass (TMB) responding by respiration to glucose addition, and the lag period (T_{lag}).

Microbial maximal specific growth rate μ was used as an intrinsic property of the microbial population to estimate the prevailing growth strategy of the microbial community. According to Blagodatskaya et al. (2010), higher μ reflects relative domination or shift towards fast-growing *r*-strategists, while lower μ values show

295 relative domination or shift towards slow-growing *K*-strategists.

296 Considering that PHBV is partially soluble in chloroform at 30°C (Jacquel et al.,
297 2007), the microbial biomass we measured by chloroform extraction may not only
298 originate from the soil but also from PHBV degradation. Therefore, microbial
299 biomass C (MBC) was determined using the initial rate of substrate-induced
300 respiration after substrate addition according to the equation of Blagodatskaya et al.
301 (2010):

302 $$MBC\ (\mu g\ g^{-1}\ soil) = (\mu l\ CO_2\ g^{-1}\ soil\ h^{-1}) \times 40.04 \quad (2)$$

303

304 *2.7 Soil bacterial community structure*

305 *2.7.1 Soil genomic DNA extraction, PCR amplification and Illumina sequencing*

306 Total DNA was extracted from 0.5 g soil for each treatment using the Mo Bio
307 PowerSoil DNA isolation kit (Qiagen Inc., Carlsbad, CA, USA) according to the
308 manufacturer's instructions. After extraction, the quality and concentration of DNA
309 were tested using a NanoDrop ND 200 spectrophotometer (Thermo Scientific, USA).
310 According to the concentration, all DNA samples were diluted to 1 ng μl^{-1} before PCR
311 amplification. We note that the DNA extracted from Control-hotspots was leaked out
312 during shipping for sequencing analysis, and then the concentration of DNA could not
313 reach to the detection threshold. Therefore, the samples from this treatment could not
314 be determined.

315 The V4 and V5 variable region of the bacterial 16S rRNA gene were amplified
316 using the primers 515F (5'-CCATCTCATCCCTGCGTGTCTCCGAC-3') and 907R
317 (5'-CCTATCCCCTGTGTGCCTTGGCAGTC-3'). The polymerase chain reaction
318 (PCR) amplification mixture was prepared with 1 μl purified DNA template (10 ng), 5

μl 10 × PCR buffer, 2.25 mmol l^{-1} $MgCl_2$, 0.8 mmol l^{-1} deoxyribonucleotide triphosphate (dNTP), 0.5 μmol l^{-1} of each primer, 2.5 U Taq DNA polymerase, and sterile filtered ultraclean water to a final volume of 50 μl. All the reactions were carried out in a PTC-200 thermal cycler (MJ Research Co., NY, USA). The PCR cycles included a 4 min initial denaturation at 94 °C, followed by 30 cycles of denaturation at 94 °C for 1 min, annealing at 53 °C for 30 s, extension at 72 °C for 1 min, and a 5-min final elongation step at 72 °C. The PCR products were quality-screened and purified by Qiagen Gel Extraction kit (Qiagen, Hilden, Germany). Next, all the amplicons were sequenced on the Illumina Miseq PE250 platform at Novogene Biotech Co., Ltd., Beijing, China. All the sequences have been submit to NCBI SRA data repository under the Accession No. PRJNA648785.

2.7.2 16S gene sequences processing

Briefly, de-noising and chimera analysis conducted with the AmpliconNoise and UCHIME algorithms were used to reduce sequence errors (Vargas-Gastelum et al., 2015). Furthermore, quality trimming was conducted to remove unwanted sequences shorter than 200 bp and reads containing ambiguous bases and with homopolymers longer than eight bases. The remaining sequences were used to identify the unique sequences by aligning with the SILVA reference database (v.128) (Quast et al., 2013). Within unique sequences, the UCHIME tool was applied to remove chimeras. Then, “Chloroplast”, “Mitochondria”, or “unknown” were identified and removed from the dataset. Subsequently, after calculating the pairwise distance and generating the distance matrix, a 97% identity threshold was used to cluster sequences into Operational Taxonomic Units (OTUs) according to the UCLUST algorithm (Edgar et al., 2011). The most abundant sequence in each OTU was picked as the representative

sequence. For each representative sequence, the SILVA reference database (v.128) was applied to annotate the taxonomic information using RDP classifier algorithm (Wang et al., 2007).

2.8 Statistical analysis

The experiment was carried out with four replicates for each parameter. All values presented in the figures are means ± standard errors of the means (mean ± SE). The enzyme kinetic parameters (V_{max} and K_m) were fitted via the non-linear regression routine of SigmaPlot (version 12.5; Systat Software, Inc., San Jose, CA, USA). The DNA data were rarefied to an equal depth within the minimum observed sample size across all the samples. The following six parameters, namely Richness, Pielou, Chao1, Shannon, Simpson, and abundance-based coverage (ACE), were calculated to describe the alpha diversity of the soil bacterial community based on OTU abundance. The calculation was conducted in QIIME 2 and the illustration was performed by R software (Ver. 3.2) using the packages “ggplot2” and “metacoder”.

Prior to the analysis of variance (ANOVA), the data were tested for normality (Shapiro-Wilk, $p > 0.05$) and homogeneity of variance (Levene-test, $p > 0.05$). Any dataset that was not normally distributed was root square or $\log_{10}$-transformed to conform with the assumption of normality before further statistical analysis. For alpha diversity index that did not conform to the assumption of normality, the nonparametric Kruskal-Wallis H-Test was applied to determine whether there were significant differences in alpha diversity among different treatments.

3. Results

3.1 Effect of PHBV on plant and soil properties

The mean plant biomass was 0.24 g pot^{-1} without microplastics addition (Table 1). However, PHBV addition ultimately resulted in plant death. PHBV addition greatly increased the soil microbial biomass and dissolved organic C content ($p < 0.05$, Table 1). MBC and DOC were 12 and 54 times higher in the PHBV-treated than in the control soil, respectively. Additionally, MBN was 45% higher in the PHBV-treatment in comparison to the control, whereas DON decreased by 66% compared to the control soil.

3.2 Effect of PHBV on soil enzyme activities

The maximum potential enzyme activities (V_{max}) were 0.6- and 5-folds higher for β-glucosidase and leucine aminopeptidase in the microplastisphere than in the rhizosphere, respectively ($p < 0.05$, Fig. 2a, b). Similarly, the substrate affinities (K_m) of β-glucosidase and leucine aminopeptidase in the microplastisphere were 1.5-2 times higher in the rhizosphere, respectively ($p < 0.05$, Fig. 2b, d). The V_{max} and K_m of β-glucosidase and leucine aminopeptidase in microplastisphere were significantly higher compared to those in the PHBV-treated bulk soil ($p < 0.05$, Fig. 2). In the bulk soil, however, none of the tested enzymes were affected by PHBV addition ($p > 0.05$, Fig. 2). Furthermore, the V_{max} of β-glucosidase was positively correlated with active microbial biomass ($R^2 = 0.7$, $p < 0.05$, Fig. S4). The catalytic efficiency (V_{max} / K_m) of leucine aminopeptidase was higher in the microplastisphere than in the rhizosphere (*p*

389 < 0.05, Fig. S2c), and the turnover time was approximately 5 times shorter in the
390 microplastisphere than in the rhizosphere soil (Fig. S2d). However, no changes in the
391 catalytic efficiency and turnover time for all the enzymes were found in the bulk soil
392 between the PHBV-treated and control soil (p > 0.05, Fig. S2). Further, the vector
393 angle was lowest in the microplastisphere compared to other soil samples (p < 0.05,
394 Fig. S7d), indicating that microbial metabolisms may be N limited.
395
396 *3.3 Effect of PHBV on soil microbial growth rate*
397 Different microbial growth patterns in response to substrate addition were
398 observed among hotspots (microplastisphere and rhizosphere) and the bulk soil with
399 and without PHBV addition (Fig. S3). The basal respiration (BR, 45 µg C g^{-1} h^{-1}) and
400 substrate-induced growth respiration (SIGR, 58 µg C g^{-1} h^{-1}) in the microplastisphere
401 were 10 times and 12 times higher relative to the rhizosphere soil, respectively (Fig.
402 3a, b). However, the BR and SIGR in the bulk soil were not affected by PHBV
403 addition compared to the control.
404 Soil respiration showed a clear response to PHBV addition both in the hotspots
405 and in bulk soil (Fig. S3). PHBV addition decreased the maximum specific growth
406 rate (μ) by 22% in the microplastisphere compared to the bulk soil (p < 0.05; Fig. 3c),
407 whereas there was no difference in μ between the microplastisphere and the
408 PHBV-treated bulk soil (p > 0.05). Despite a slower specific growth rate, a 6-fold
409 increase in the fraction of active microbial biomass, and a four times shorter lag
410 period was observed in the microplastisphere vs. rhizosphere soil (Fig. 3d,e,f).

411

412 *3.4 Effect of PHBV on soil bacterial community composition and diversity*

413 The dominant bacteria phyla were *Actinobacteria, Proteobacteria, Acidobacteria,*
414 *Firmicutes, Bacteroidetes, Chloroflexi, Thaumarchaeota,* and *Germmatimonadetes* in
415 all treatment soils (Fig. 4A), which together encompassed ca. 96-98% of the bacterial
416 reads. Although the dominant phyla in all soils were consistent, changes in the relative
417 abundances of the dominant taxa were observed across the treatments. There was a
418 higher abundance of *Proteobacteria* and *Acidobacteria* and a lower abundance of
419 *Firmicutes* in soils with PHBV addition comparing with control treatment ($p < 0.05$,
420 Fig. 4A). In the family level, the fraction of these 20 dominant families with highest
421 relative abundance decreased after PHBV addition (Fig. 4B). Specifically, the addition
422 of PHBV induced the decrease of *Planococcaceae, Xanthomonadaceae, Bacillaceae*
423 and the increase of *Chitinophagaceae*, *Comamonadaceae* and *Oxalobacteraceae* (Fig.
424 4B). The detailed family level changes of bulk and hotspot soil bacterial community
425 induced by PHBV addition were also given in Figure 5C. Of the 3800 OTUs detected
426 across all samples, the major numbers of OTUs (n = 3622) were shared by
427 control-bulk, PHBV-bulk, and PHBV-hotspots soils, while 54 OTUs were unique to
428 PHBV-hotspots soil and 16 OTUs were unique to the PHBV-bulk soil (Fig. 5A).

429 The mean values for ACE, Chao1, Richness, and Shannon indices in the
430 PHBV-treated bulk soil increased by 10%, 11%, 16%, and 18% relative to the control
431 soil, respectively (Fig. S5), while there were no differences between the
432 microplastisphere and bulk soil after PHBV addition ($p > 0.05$).

4. Discussion

4.1 Effect of PHBV on plant growth

PHBV in a polymeric or monomeric state is generally viewed as having very low cytotoxicity (Napathorn, 2014). In all the rhizoboxes added with PHBV, however, all the plants eventually died during the 4-week experiment. This is consistent with previous reports showing that degradation of conventional and bio-based microplastics might negatively affect plant growth when present at high concentrations (Qi et al., 2018; Qi et al., 2020b; Zang et al., 2020). Given that bioplastic polymers are solely composed of C, O and H, it is likely that PHBV addition to soil induced microbial immobilization of essential nutrients (e.g., N, P) leading to increased plant stress (Volova et al., 2017; Boots et al., 2019). Such an N immobilization was further confirmed by the decreased DON but increased MBN in PHBV-added soil compared to the unamended control treatment (Table 1). This is consistent with Sander (2019) who found that microorganisms on the surface of microplastics need to acquire N from the surrounding soil to fuel growth. It also suggests that PHBV may have stimulated opportunistic plant pathogens (Matavulj et al., 1992), however, more work is required to confirm this. An alternative explanation might be that PHBV induced phytotoxicity due to acidification of the soil because of the release of high concentrations of 3-hydroxybutyric acid during PHBV degradation. However, this would normally differentially affect root growth rather than shoot growth (Lucas et al., 2008). Further, based on the degradation of other biopolymers

455 (e.g. cellulose, proteins), it is unlikely that an accumulation of the monomer will
456 occur due to rapid microbial consumption (Jan et al., 2009). This is quite likely as it is
457 the monomer which is naturally present as a microbial storage compound
458 (Mason-Jones et al. 2019). However, it is possible that undisclosed additives or
459 contaminants in the polymer might also have induced phytotoxicity (Zimmermann et
460 al., 2019). Lastly, we cannot discount other general changes in soil properties and
461 microbial communities following PHBV addition which may also have inhibited plant
462 growth, contributing to plant death (Saarma et al., 2003; Wen et al., 2020). We
463 conclude, that contrary to expectation, commercially-sourced PHBV was deleterious
464 to plant growth, at least under higher concentrations of PHBV in the short term, as
465 indicated by the lower seed germination over 7-days germination (Fig. S6). Further
466 experiments are therefore needed to determine the mechanistic basis of this response.
467
468 *4.2 Effect of PHBV on soil microbial and enzymatic functional traits*
469 Soil enzyme production is sensitive to both energy and nutrient availability
470 (Allison et al., 2011). This tenet was supported in our study where the input of labile
471 C (i.e. PHBV) increased enzyme activities in hotspots by up to 2 times compared to
472 the bulk soil. This increase in microbial activity is unsurprising given that
473 poly-3-hydroxybutyrate is a common storage compound produced by a wide range of
474 taxonomically different groups of microorganisms, particularly in response to N
475 deficiency and cold stress (Obruca et al., 2016). Consequently, the ability to use
476 PHBV-C is expected to be a widespread trait within the microbial community. For C-

and N-degrading enzymes, the activity difference between hotspots and the bulk soil was 2-10 times larger when PHBV was added (Fig. 2a, c), demonstrating that bioplastic incorporation into the soil directly influences C and N cycling. The higher V_{max} of β-glucosidase in the microplastisphere versus rhizosphere soil can be attributed to the faster growing biomass after PHBV addition (Fig. 3e). This is supported by the positive correlation between our measurement of the active microbial biomass and the V_{max} of β-glucosidase (R^2 = 0.7, Fig. S4). The increase in β-glucosidase also suggests that PHBV is stimulating the breakdown of other common soil polymers (i.e. cellulose). Further, PHBV could be broken down by depolymerases releasing hydroxybutyric acid monomers which fuel the production of energetically expensive exoenzymes (i.e. leucine aminopeptidase; Fig. 2c) capable of degrading SOM to acquire N for growth (i.e. positive priming; Zang et al., 2016; Zhou et al., 2020a, b). This was supported by a higher BR and SIGR in the microplastisphere relative to the bulk soil (Fig. 3a, b), as well as the wider ratio of DOC and DON in the PHBV-treated soil (294) than in the control soil (1.77) (Table. 1). In accordance with previous studies, N limitation also induced an increase in the catalytic properties (K_a) of leucine aminopeptidase (Song et al., 2020). In line with this, the much shorter turnover time of substrates and higher K_a of leucine aminopeptidase in the microplastisphere was observed compared to the rhizosphere (Fig. S2c,d), which suggests that the community was more limited by N than P in the microplastisphere. This could be supported by lower proportional activity of C- to N-cycling enzymes but higher proportional activity of C- to P-cycling enzymes in the

499 microplastisphere versus the rhizosphere (Fig. S7). The lower vector angle in the
500 microplastisphere further confirmed the microbial metabolisms were likely limited by
501 soil N. We therefore hypothesize that due to N limitation the microbial community
502 either (i) changed the intrinsic properties of their hydrolytic enzymes to adapt to the
503 presence of the C-rich bioplastic, and/or (ii) that PHBV induced a shift in the soil
504 microbial community and thus the types of enzymes being produced (Kujur and Patel,
505 2013). Overall, we conclude that N limitation is connected with microbial N
506 immobilization due to stimulated microbial growth after C supply from PHBV
507 addition. The C input from the catabolism of PHBV will increase microbial biomass
508 and intensify the N limitation. This was supported by the increased MBC and enzyme
509 activities (especially N related), as well as the shift in enzymatic stoichiometric ratio
510 and bacterial community. This contrasts with C hotpots in the rhizosphere, where the
511 supply of C is probably less and where N is also lost from root epidermal cells in the
512 form of amino acids providing a more balanced nutrient supply to the microbial
513 community (Jones et al., 2009).

514 Here we speculate that PHBV breakdown was initially limited by the availability
515 of polyhydroxybutyrate depolymerase (Jendrossek et al., 1993). The abundance and
516 level of expression of this enzyme in soil remains unknown, however, an NCBI search
517 revealed its presence in a wide range of microbial taxa. Although PHB depolymerase
518 may be internally targeted (i.e. to break down internal storage C), there is also a large
519 amount of evidence that it can be externally targeted (i.e. be an exoenzyme;
520 Jendrossek and Handrick, 2002), probably to degrade microbial necromass (Handrick

et al., 2004). Our data support the view that PHBV can be used as a sole C substrate by the bacterial community when supplied exogenously (Martinez-Tobon et al., 2018). However, we also observed a significant decrease (22%) in microbial specific growth rate μ in the microplastisphere compared to the rhizosphere, indicating the potential dominance of *K*-strategy microorganisms. *K*-strategists typically store more C in their cells and consume it slower (Nguyen and Guckert, 2001), lowering respiration rates. We therefore hypothesize that PHBV degraders break down PHBV exogenously into monomeric units which can then be subsequently transported into the cell where re-polymerization into PHB occurs (Shen et al., 2015). Consequently, microbial community structure in the microplastisphere shifted toward species with a lower affinity to oligosaccharides and peptides indicated by a higher K_m of β-glucosidase and leucine aminopeptidase.

4.3. Effect of PHBV on soil bacterial community structure

PHBV addition was associated with an increase in the relative abundance of *Acidobacteria* and *Chloroflexi*, and a decrease in the relative abundance of *Firmicutes*, The latter have previously been described as fast-growing copiotrophs that thrive in environments of high C availability (Cleveland et al., 2007; Jenkins et al., 2010). In contrast, *Acidobacteria* and *Chloroflexi* tend to dominate in oligotrophic environments where N availability is low (Ho et al., 2017). *Nitrospirae* are nitrite-oxidizing bacteria that are ubiquitous in terrestrial environments and that play a major role in biological N cycling and nitrification in agricultural soils (Xia et al.,

2011). The higher abundance of *Nitrospirae* after PHBV addition indicated a change in N cycling (Zecchin et al., 2018), which was attributed to greater nutrient limitation in the microplastisphere than in the bulk soil (as indicated by V_{max} ratio of C-to-N cycling enzymes; 5.1 vs. 8.6) (Table S1). The relative proportion of *Bacteroidetes* also increased in the PHBV treatments. These largely copiotrophic organisms are widely distributed in soils, and are considered to be specialized in degrading complex organic matter (Huang et al., 2019). Thus, DOM pools increased in the PHBV-treated soil compared with bulk soil due to the release of monomeric compounds from PHBV degradation (Table 1). Although only bacterial communities were investigated in this study, it is likely that fungi and mesofauna populations are also greatly affected by PHBV addition and involved in its degradation. Further studies are required to gain a better insight into the complex interactions between these groups. Overall, our results highlight the potential of PHBV to trigger metabolic changes in soil microorganisms (Fig. 6), and thus potentially impact their functional role in soil (Huang et al., 2019). In addition to the microplastisphere, PHBV addition also changed the microbial community in the bulk soil, suggesting that these changes are not only confined to hotspots in the soil.

Conclusion

Microbial activity in agricultural soil is typically C-limited, such that even small C inputs can induce metabolic changes in the soil microbial community. Here we clearly showed that PHBV addition increased microbial activity, growth, and

exoenzyme activity. This most likely leads to the enhanced mineralization of native SOM by co-metabolism, i.e. microorganisms degrade SOM by using degradable polymers (i.e. hydroxybutyric acid molecules) as an energy source. Remarkably, greater enzyme activity and microbial biomass, and lower affinity for the substrate were observed in the microplastisphere compared to the rhizosphere, indicating a stronger and faster C and nutrient turnover with PHBV addition in hotspots. Taken together, the unique environment may benefit microbial survival in PHBV-treated soil compared with the rhizosphere, possibly altering the soil ecological functions and biogeochemical processes, which may result in a stimulation of soil C and nutrients cycling. Although bioplastics have been heralded as a solution to petroleum-based plastics, our research indicates that it is also important to consider the potential disbenefits of bioplastics, e.g., for plant growth and health. This is exemplified in the use of plastic microbeads in cosmetics and plastic mulch films in agriculture where the negative environmental consequences were only realized decades after their introduction (Sintim and Flurt, 2017; Qi et al., 2020b). Our research was designed to understand the short-term impact of a localized PHBV hotspot in soil. It is clear, however, that longer-term field-scale studies are also required. In-field testing of biodegradation of PHBV under different scenarios (e.g., soil types, agricultural practice, climate changes) as well as using a realistic mixture of polymers over longer periods is therefore required, with particular attention to plant-soil-microbial interactions.

Acknowledgements

This work was supported by the China Agriculture Research System (CARS07-B-5) and the UKRI Global Challenges Research Fund (GCRF) project awarded to Bangor University (NE/V005871/1). We also would like to thank the UK-China Virtual Joint Centre for Agricultural Nitrogen (CINAg, BB/N013468/1), which is jointly supported by the Newton Fund, via UK Biotechnology and Biological Sciences Research Council and Natural Environment Research Council, and the Chinese Ministry of Science and Technology. Jie Zhou would like to thank the support from the China Scholarship Council (CSC). Heng Gui would like to thank the National Natural Science Foundation of China (NSFC Grant 32001296) and Yunnan Fundamental Research Projects (Grant No. 2019FB063). The authors would like to thank Karin Schmidt for her laboratory assistance. The authors also thank the editor and two anonymous reviewers for their insightful comments.

600 **References**

601 Allison, S.D., Weintraub, M.N., Gartner, T.B., Waldrop, M.P., 2011. Evolutionary
602 economic principles as regulators of soil enzyme production and ecosystem
603 function. In: Shukla, G., Varma, A. (Eds.), Soil Enzymology. Springer, Berlin,
604 229-244.

605 Barnard, R.L., Osborne, C.A., Firestone, M.K., 2013. Responses of soil bacterial and
606 fungal communities to extreme desiccation and rewetting. The ISME Journal 7,
607 2229-2241.

608 Blagodatskaya, E., Blagodatsky, S., Dorodnikov, M., Kuzyakov, Y., 2010. Elevated
609 atmospheric CO_2 increases microbial growth rates in soil: results of three CO_2
610 enrichment experiments. Global Change Biology 16, 836-848.

611 Boots, B., Russell, C.W., Green, D.S., 2019. Effects of microplastics in soil
612 ecosystems: above and below ground. Environmental Science and Technology
613 53, 11496-11506.

614 Bugnicourt, E., Cinelli, P., Lazzeri, A., Alvarez, V., 2014. Polyhydroxyalkanoate
615 (PHA): Review of synthesis, characteristics, processing and potential
616 applications in packaging. Express Polymer Letters 8, 791-808.

617 Cleveland, C.C., Nemergut, D.R., Schmidt, S.K., Townsend, A.R., 2007. Increases in
618 soil respiration following labile carbon additions linked to rapid shifts in soil
619 microbial community composition. Biogeochemistry 82, 229–240.

620 Davidson, E.A., Janssens, A., 2006. Temperature sensitivity of soil carbon
621 decomposition and feedbacks to climate change. Nature 440, 165-173.

622 de Souza Machado, A.A., Lau, C.W., Kloas, W., Bergmann, J., Bachelier, J.B., Faltin,
623 E., Becker, R., Görlich, A.S., Rillig, M.C., 2019. Microplastics can change soil
624 properties and affect plant performance. Environmental Science and Technology
625 53, 6044-6052.
626 Duis, K., Coors, A., 2016. Microplastics in the aquatic and terrestrial environment:
627 sources (with a specific focus on personal care products), fate and effects.
628 Environmental Sciences Europe 28, 2-8.
629 Edgar, R.C., Haas, B.J., Clemente, J.C., Quince, C., Knight, R., 2011. UCHIME
630 improves sensitivity and speed of chimera detection. Bioinformatics 27,
631 2194-2200.
632 Fei, Y., Huang, S., Zhang, H., Tong, Y., Wen, D., Xia, X., Wang, H., Luo, Y.,
633 Barceló, D., 2020. Response of soil enzyme activities and bacterial communities
634 to the accumulation of microplastics in an acid cropped soil. Science of the Total
635 Environment 707, 135634.
636 Fuller, S., Gautam, A., 2016. Procedure for measuring microplastics using Pressurized
637 Fluid Extraction. Environmental Science and Technology 50, 5774-5780.
638 Garrison, T.F., Murawski, A., Quirino, R.L., 2016. Bio-based polymers with potential
639 for biodegradability. Polymers 8, 262.
640 Geisseler, D., Horwath, W.R., 2009. Short-term dynamics of soil carbon, microbial
641 biomass, and soil enzymes activities as compared to long-term effects of tillage
642 in irrigated row crops. Biology and Fertility of Soils 46, 65-72.

643 German, D., Weintraub, M., Grandy, A., Lauber, C., Rinkes, Z., Allison, S., 2011.
644 Optimization of hydrolytic and oxidative enzyme methods for ecosystem studies.
645 Soil Biology and Biochemistry 43, 1387-1397.
646 Gross, R.A., Kalra, B., 2002. Biodegradable polymers for the environment. Science
647 297, 803–807.
648 Haider, T.P., Völker, C., Kramm, J., Landfester, K., Wurm, F.R., 2019. Plastics of the
649 Future? The impact of biodegradable polymers on the environment and on
650 society. Angewandte Chemie 58, 50-62.
651 Handrick, R., Reinhardt, S., Kimmig, P., Jendrossek, D., 2004. The "intracellular"
652 poly(3-hydroxybutyrate) (PHB) depolymerase of *Rhodospirillum rubrum* is a
653 periplasm-located protein with specificity for native PHB and with structural
654 similarity to extracellular PHB depolymerases. Journal of Bacteriology 186,
655 7243-7253.
656 Hausmann, B., Knorr, K.H., Schreck, K., Tringe, S.G., Glavina del Rio, T., Loy, A.,
657 Pester, M., 2016. Consortia of low-abundance bacteria drive sulfate
658 reduction-dependent degradation of fermentation products in peat soil
659 microcosms. The ISME Journal 10, 2365–2375.
660 Hoang, D.T., Maranguit, D., Kuzyakov, Y., Razavi, B.S., 2020. Accelerated microbial
661 activity, turnover and efficiency in the drilosphere is depth dependent. Soil
662 Biology and Biochemistry 147, 107852.
663 Huang, Y., Zhao, Y., Wang, J., Zhang, M., Jia, W., Qin, X., 2019. LDPE microplastics
664 films alter microbial community composition and enzymatic activities in soil.

665 Environmental Pollution 254, 112983.
666 Jacquel, N., Lo, C.W., Wu, H.S., Wei, Y.H., Wang, S.S., 2007. Solubility of
667 polyhydroxyalkanoates by experiment and thermodynamic correlations. AIChE
668 Journal 53, 2704-2714.
669 Jambeck, J.R., Geyer, R., Wilcox, C., Siegler, T.R., Perryman, M., Andrady, A.,
670 Narayan, R., Law, K.L., 2015. Plastic waste inputs from land into the ocean.
671 Science 347, 768–771.
672 Jan, M.T., Roberts, P., Tonheim, S.K., Jones, D.L., 2009. Protein breakdown
673 represents a major bottleneck in nitrogen cycling in grassland soils. Soil Biology
674 and Biochemistry 41, 2272-2282.
675 Jendrossek, D., Handrick, R., 2002. Microbial degradation of polyhydroxyalkanoates.
676 Annual Review of Microbiology 56, 403-432.
677 Jendrossek, D., Knoke, I., Habibian, R.B., Steinbüchel, A., Schlegel, H.G., 1993.
678 Degradation of poly(3-hydroxybutyrate), PHB, by bacteria and purification of a
679 novel PHB depolymerase from *Comamonas* sp. Journal of Environmental
680 Polymer Degradation 1, 53-63.
681 Jenkins, S.N., Rushton, S.P., Lanyon, C.V., Whiteley, A.S., Waite, I.S., Brookes, P.C.,
682 Kemmitt, S., Evershed, R.P., O'Donnell, A.G., 2010. Taxon-specific responses of
683 soil bacteria to the addition of low level C inputs. Soil Biology and Biochemistry
684 42, 1624–163.
685 Jiang, Y., Chen, Y., Zheng, X., 2009. Efficient polyhydroxyalkanoates production
686 from a waste-activated sludge alkaline fermentation liquid by activated sludge

687 submitted to the aerobic feeding and discharge process. Environmental Science
688 and Technology 43, 7734-7741.
689 Jones, D.L., Nguyen, C., Finlay, R.D., 2009. Carbon flow in the rhizosphere: carbon
690 trading at the soil-root interface. Plant and Soil 32, 5-33.
691 Kujur, M., Patel, A.K., 2013. Kinetics of soil enzyme activities under different
692 ecosystems: an index of soil quality. Chilean Journal of Agricultural Research 74,
693 96-104.
694 Kuzyakov, Y., 2010. Priming effects: interactions between living and dead organic
695 matter. Soil Biology and Biochemistry 42, 1363-1371.
696 Kuzyakov, Y., Blagodatskaya, E., 2015. Microbial hotspots and hot moments in soil:
697 Concept & review. Soil Biology and Biochemistry 83, 184-199.
698 Lammirato, C., Miltner, A., Wick, L.Y., Kästner, M., 2010. Hydrolysis of cellobiose
699 by β-glucosidase in the presence of soil minerals - interactions at solid - liquid
700 interfaces and effects on enzyme activity levels. Soil Biology and Biochemistry
701 42, 2203-2210.
702 Liu, S., Razavi, B.S., Su, X., Maharjan, M., Zarebanadkouki, M., Blagodatskaya, E.,
703 Kuzyakov, Y., 2017. Spatio-temporal patterns of enzyme activities after manure
704 application reflect mechanisms of niche differentiation between plants and
705 microorganisms. Soil Biology and Biochemistry 112, 100-109.
706 Lucas, N., Bienaime, C., Belloy, C., Queneudec, M., Silvestre, F., Nava-Saucedo, J.,
707 2008. Polymer biodegradation: mechanisms and estimation techniques.
708 Chemosphere 73, 429-442.

709 Lopez-Hernandez, D., Lavelle, P., Niño, M., 1993. Phosphorus transformations in two
710 P-sorption contrasting tropical soils during transit through *Pontoscolex*
711 *corethrurus* (Glossoscolecidae: Oligochaeta). Soil Biology and Biochemistry 25,
712 789-792.
713 Mason-Jones, K., Banfield, C.C., Dippold, M.A., 2019. Compound-specific ^{13}C stable
714 isotope probing confirms synthesis of polyhydroxybutyrate by soil bacteria.
715 Rapid Communications in Mass Spectrometry 33, 795-802.
716 Martinez-Tobon, D.I., Gul, M., Elias, A.L., Sauvageau, D., 2018.
717 Polyhydroxybutyrate (PHB) biodegradation using bacterial strains with
718 demonstrated and predicted PHB depolymerase activity. Applied Microbiology
719 and Biotechnology 102, 8049-8067.
720 Matavulj, M., Molitoris, H.P., 1992. Fungal degradation of polyhydroxyalkanoates
721 and a semiquantitative assay for screening their degradation by terrestrial fungi.
722 FEMS Microbiology Letters 103, 323-331.
723 Marx, M., Wood, M., Jarvis, S., 2001. A fluorimetric assay for the study of enzyme
724 diversity in soils. Soil Biology and Biochemistry 33, 1633-1640.
725 Meng, K., Ren, W., Teng, Y., Wang, B., Han, Y., Christie, P., Luo Y., 2019.
726 Application of biodegradable seedling trays in paddy fields: impacts on the
727 microbial community. Science of the Total Environment 656, 750-759.
728 Moorhead, D.L., Sinsabaugh, R.L., Hill, B.H., Weintraub, M.N., 2016. Vector analysis
729 of ecoenzyme activities reveal constraints on coupled C, N and P dynamics. Soil
730 Biology and Biochemistry 93, 1-7.

731 Napathorn, S.C., 2014. Biocompatibilities and biodegradation of
732 poly(3-hydroxybutyrate-co-3-hydroxyvalerate)s produced by a model metabolic
733 reaction-based system. BMC Microbiology 14, 285.
734 Nguyen, C., Guckert, A., 2001. Short-term utilisation of ^{14}C-glucose by soil
735 microorganisms in relation to carbon availability. Soil Biology and Biochemistry
736 33, 53-60.
737 Obruca, S., Sedlacek, P., Krzyzanek, V., Mravec, F., Hrubanova, K., Samek, O.,
738 Kucera, D., Benesova, P., Marova, I., 2016. Accumulation of
739 poly(3-hydroxybutyrate) helps bacterial cells to survive freezing. PloS One 11,
740 e0157778.
741 Petersen, B.M., Berntsen, J., Hansen, S., Jensen, L.S., 2005. CN-SIM a model for the
742 turnover of soil organic matter. I. Long-term carbon and radiocarbon
743 development. Soil Biology and Biochemistry 37, 359–374.
744 Qi, R., Jones, D.L., Li, Z., Liu, Q., Yan, C., 2020a. Behavior of microplastics and
745 plastic film residues in the soil environment: A critical review. Science of the
746 Total Environment, 703, 134722.
747 Qi, Y.L., Yang, X.M., Pelaez, A.M., Lwanga, E.H., Beriot, N., Gertsen, H., Garbeva,
748 P., Geissen, V., 2018. Macro- and micro- plastics in soil-plant system: Effects of
749 plastic mulch film residues on wheat (*Triticum aestivum*) growth. Science of the
750 Total Environment 645, 1048-1056.
751 Qi, Y., Ossowicki, A., Yang, X., Huerta Lwanga, E., Dini-Andreote, F., Geissen, V.,
752 Garbeva, P., 2020b. Effects of plastic mulch film residues on wheat rhizosphere
753 and soil properties. Journal of Hazardous Materials, 387, 121711.
754 Quast, C., Pruesse, E., Yilmaz, P., Gerken, J., Schweer, T., Yarza, P., Peplies, J., &
755 Glöckner, F. O., 2013. The SILVA ribosomal RNA gene database project:

improved data processing and web-based tools. Nucleic Acids Research, 41, 590-596.

Razavi, B.S., Zarebanadkouki, M., Blagodatskaya, E., Kuzyakov, Y., 2016. Rhizosphere shape of lentil and maize: spatial distribution of enzyme activities. Soil Biology and Biochemistry 96, 229-237.

Rillig, M.C., 2012. Microplastic in terrestrial ecosystems and the soil? Environmental Science & Technology 46, 6453–6454.

Rivera-Briso, A.L., Serrano-Aroca, Á., 2018. Poly(3-hydroxybutyrate-co-3-hydroxyvalerate): Enhancement strategies for advanced applications. Polymers 10, 732.

Rochman, C.M., 2018. Microplastics research-from sink to source. Science 360, 28-29.

Saarma, K., Tarkka, M.T., Itavaara, M., Fagerstedt, K.V., 2003. Heat shock protein synthesis is induced by diethyl phthalate but not by di(2-ethylhexyl) phthalate in radish (*Raphanus sativus*). Journal of Plant Physiology 160, 1001–1010.

Sander, M., 2019. Biodegradation of polymeric mulch films in agricultural soils: Concepts, knowledge gaps, and future research directions. Environmental Science and Technology 53, 2304-2315.

Shen, Y.C., Shaw, G.C., 2015. A membrane transporter required for 3-hydroxybutyrate uptake during the early sporulation stage in *Bacillus subtilis*. FEMS Microbiology Letters 362, UNSP fnv165.

Sintim, H.Y., Flury, M., 2017. Is biodegradable plastic mulch the solution to agriculture's plastic problem? Environmental Science & Technology 51, 1068-1069.

780 Song, X., Razavi, B., Ludwig, B., Zamanian, K., Zang, H., Kuzyakov, Y., Dippold,
781 M., Gunina, A., 2020. Combined biochar and nitrogen application stimulates
782 enzyme activity and root plasticity. Science of the Total Environment 735,
783 139393.
784 Steinmetz, Z., Wollmann, C., Schaefer, M., Buchmann, C., David, J., Troger, J.,
785 Munoz, K., Fror, O., Schaumann, G.E., 2016. Plastic mulching in agriculture.
786 Trading short-term agronomic benefits for -term soil degradation? Science of the
787 Total Environment 550, 690-705.
788 Vargas-Gastelum, L., Romero-Olivares, A.L., Escalante, A.E., Rocha-Olivares, A.,
789 Brizuela, C., Riquelme, M., 2015. Impact of seasonal changes on fungal diversity
790 of a semi-arid ecosystem revealed by 454 pyrosequencing. FEMS Microbiology
791 Ecology 91, fiv044.
792 Volova, T.G., Prudnikova, S.V., Vinogradova, O.N., Syrvacheva, D.A., Shishatskaya,
793 E.I., 2017. Microbial degradation of polyhydroxyalkanoates with different
794 chemical compositions and their biodegradability. Microbial Ecology 73,
795 353-367.
796 Wang, Q., Garrity, G.M., Tiedje, J.M., Cole, J.R., 2007. Naive Bayesian classifier for
797 rapid assignment of rRNA sequences into the new bacterial taxonomy. Applied
798 and Environmental Microbiology 73, 5261-5267.
799 Weithmann, N., Möller, J.N., Löder, M.G., Piehl, S., Laforsch, C., Freitag, R., 2018.
800 Organic fertilizer as a vehicle for the entry of microplastic into the environment.
801 Science Advances 4, 8060.
802 Wen, Y., Zang, H., Ma, Q., Evans, C.D., Chadwick, D.R., Jones, D.L., 2019. Is the
803 ‘enzyme latch’ or ‘iron gate’ the key to protecting soil organic carbon in
804 peatlands? Geoderma 349, 107-113.

Wen, Y., Freeman, B., Ma, Q., Evans, C., Chadwick, D., Zang, H., Jones, D., 2020. Raising the groundwater table in the non-growing season can reduce greenhouse gas emissions and maintain crop productivity in cultivated fen peats. Journal of Cleaner Production 262, 121179.

Wright, S.L., Kelly, F.J., 2017. Plastic and human health: a micro issue? Environmental Science & Technology 51, 6634-6647.

Xia, W., Zhang, C., Zeng, X., Feng, Y., Weng, J., Lin, X., 2011. Autotrophic growth of nitrifying community in an agricultural soil. The ISME Journal 5, 1226-1236.

Zang, H.D., Blagodatskaya, E., Wang, J.Y., Xu, X.L., Kuzyakov, Y., 2017. Nitrogen fertilization increases rhizodeposit incorporation into microbial biomass and reduces soil organic matter losses. Biology and Fertility of Soils 53, 419-429.

Zang, H, Blagodatskaya, E, Wen, Y, Xu, X, Kuzyakov, Y, 2018. Carbon sequestration and turnover in soil under the energy crop Miscanthus: repeated ^{13}C natural abundance approach and literature synthesis. Global Change Biology Bioenergy 10, 262-271.

Zang, H., Wang, J., Kuzyakov, Y., 2016. N fertilization decreases soil organic matter decomposition in the rhizosphere. Applied Soil Ecology 108, 47-53.

Zang, H, Xiao, M, Wang, Y, Ling, N, Wu, J, Ge, T, Kuzyakov, Y, 2019. Allocation of assimilated carbon in paddies depending on rice age, chase period and N fertilization: experiment with $^{13}CO_2$ labelling and literature synthesis. Plant and Soil 445, 113-123.

Zang, H., Zhou, J., Marshall, M.R., Chadwick, D.R., Wen, Y., Jones, D.L., 2020. Microplastics in the agroecosystem: Are they an emerging threat to the plant-soil system? Soil Biology and Biochemistry 148, 107926.

829 Zecchin, S., Mueller, R.C., Seifert, J., Stingl, U., Anantharaman, K., von Bergen, M.,
830 Cavalca, L., Pester, M., 2018. Rice paddy Nitrospirae carry and express genes
831 related to sulfate respiration: proposal of the new genus "Candidatus Sulfobium".
832 Applied and Environmental Microbiology 84, e02224-17.
833 Zettler, E.R., Mincer, T.J., Amaral-Zettler, L.A., 2013. Life in the "plastisphere":
834 microbial communities on plastic marine debris. Environmental Science and
835 Technology 47, 7137-7146.
836 Zhang, X., Kuzyakov, Y., Zang, H., Dippold, M.A., Shi, L., Spielvogel, S., Razavi,
837 B.S., 2020. Rhizosphere hotspots: root hairs and warming control microbial
838 efficiency, carbon utilization and energy production. Soil Biology and
839 Biochemistry 107872.
840 Zimmermann, L., Dierkes, G., Ternes, T.A., Volker, C., Wagner, M., 2019.
841 Benchmarking the in vitro toxicity and chemical composition of plastic
842 consumer products. Environmental Science & Technology 53, 11467-11477.
843 Zhou, J., Wen, Y., Shi, L.L., Marshall, M.R., Kuzyakov, Y., Blagodatskaya, E., Zang,
844 H.D., 2020a. Strong priming of soil organic matter induced by frequent input of
845 labile carbon. Soil Biology and Biochemistry 152, 108069.
846 Zhou, J., Zang, H., Loeppmann, S., Gube, M., Kuzyakov, Y., Pausch, J., 2020b.
847 Arbuscular mycorrhiza enhances rhizodeposition and reduces the rhizosphere
848 priming effect on the decomposition of soil organic matter. Soil Biology and
849 Biochemistry 140, 107641.
850 Zinn, M., Witholt, B., Egli, T., 2001. Occurrence, synthesis and medical application of
851 bacterial polyhydroxyalkanoate. Advanced Drug Delivery Reviewers 253, 5-21.

852 **Table 1** Plant biomass, microbial biomass carbon (MBC) and nitrogen (MBN), and
853 dissolved organic carbon (DOC) and nitrogen (DON) in untreated soil (Control) and
854 soil to which the bioplastic poly(3-hydroxybutyrate-*co*-3-hydroxyvalerate) (PHBV)
855 was added. Values are means (± SE) of four replicates. Letters show significant
856 differences between treatments ($p < 0.05$). MBC was calculated by substrate-induced
857 growth respiration (according to Eqn (8)), MBN, DOC and DON was measured by
858 chloroform-fumigation extraction.
859

Treatment	Plant biomass (g DM pot^{-1})	MBC (mg kg^{-1})	MBN (mg kg^{-1})	DOC (mg kg^{-1})	DON (mg kg^{-1})
Control	0.24±0.02	131±23b	20.6±3.4b	163±20b	93.9±5.5a
PHBV	n.d.	1723±625a	30.4±5.6a	9049±889a	32.3±5.2b

860
861 n.d.: no data due to plant death.

862 **Figure captions**

863 **Fig. 1** Zymograms and hotspots of β-glucosidase (BG), acid phosphatase (ACP) and
864 leucine aminopeptidase (LAP) in untreated soil (Control) and soil to which the
865 bioplastic poly(3-hydroxybutyrate-*co*-3-hydroxyvalerate) (PHBV) was added. The
866 color scale bars are proportional to the enzyme activities (nmol cm^{-2} h^{-1}). The
867 zymograms are representative of 4 independent replicates. The corresponding area of
868 hotspots relative to the total area of the rhizobox for each enzyme is shown in the
869 right-hand panel. Values are means (± SE) of four replicates. Different letters show
870 significant differences between treatments ($p < 0.05$). Here, 1, 2, 3 indicate
871 rhizosphere, microplastisphere, and bulk soil.

872

873 **Fig. 2** Potential enzyme activities (V_{max}) and substrate affinities (K_m) of β-glucosidase
874 (BG), leucine aminopeptidase (LAP), and acid phosphatase (ACP) in bulk and
875 hotspots in untreated soil (Control) and soil to which the bioplastic
876 poly(3-hydroxybutyrate-*co*-3-hydroxyvalerate) (PHBV) was added. Values are means
877 (± SE) of four replicates. Different letters show significant differences between
878 treatments ($p < 0.05$).

879

880 **Fig. 3** Basal respiration (BR), substrate-induced growth respiration (SIGR), specific
881 growth rate (μ), total microbial biomass (TMB), the fraction of growing microbial
882 biomass to total microbial biomass (GMB/TMB), and their lag time in bulk and
883 hotspots in untreated soil (Control) and soil to which the bioplastic

poly(3-hydroxybutyrate-*co*-3-hydroxyvalerate) (PHBV) was added. Values are means (± SE) of four replicates. Letters show significant differences between treatments ($p < 0.05$).

Fig. 4 Stacked bar chart of the top 10 bacterial phyla with the largest mean relative abundance in untreated soil (Control-bulk), and bulk (PHBV-bulk) and hotspots (PHBV-hotspots) soils with the bioplastic poly (3-hydroxybutyrate-*co*-3-hydroxyvalerate) (PHBV) addition (A). Stacked bar plot of the 20 families with largest mean relative abundance in all soil samples (B).

Fig. 5 Venn diagram shows shared number of OTUs by untreated soil (Control-bulk), and bulk (PHBV-bulk) and hotspots (PHBV-hotspots) soils with the bioplastic poly (3-hydroxybutyrate-*co*-3-hydroxyvalerate) (PHBV) addition (A). The taxonomical information for each node was given in an individual enlarged heatmap (B). Metacoder heatmap to family level across different treatment. Each node from the center (Kingdom) to outward (Family) represents different taxonomical levels (C). The map is weighted and colored-coded based on read abundance.

Fig. 6 Conceptual diagram showing changes of microbial activities and functions in the hotspots as affected by poly(3-hydroxybutyrate-*co*-3-hydroxyvalerate) (PHBV) addition. Vertical and horizontal red arrows indicate either an increase or no change of microbial exoenzyme kinetics and functions in the hotspots compared to the bulk soil,

906 respectively. The red and orange gradient between the panels indicates the decreasing
907 trend in enzyme activity (V_{max}) and substrate affinity (K_m), respectively between the
908 microplastisphere and the rhizosphere. The blue gradient indicates the increasing
909 trend in microbial specific growth rate (μ).

910

911 Fig. 1

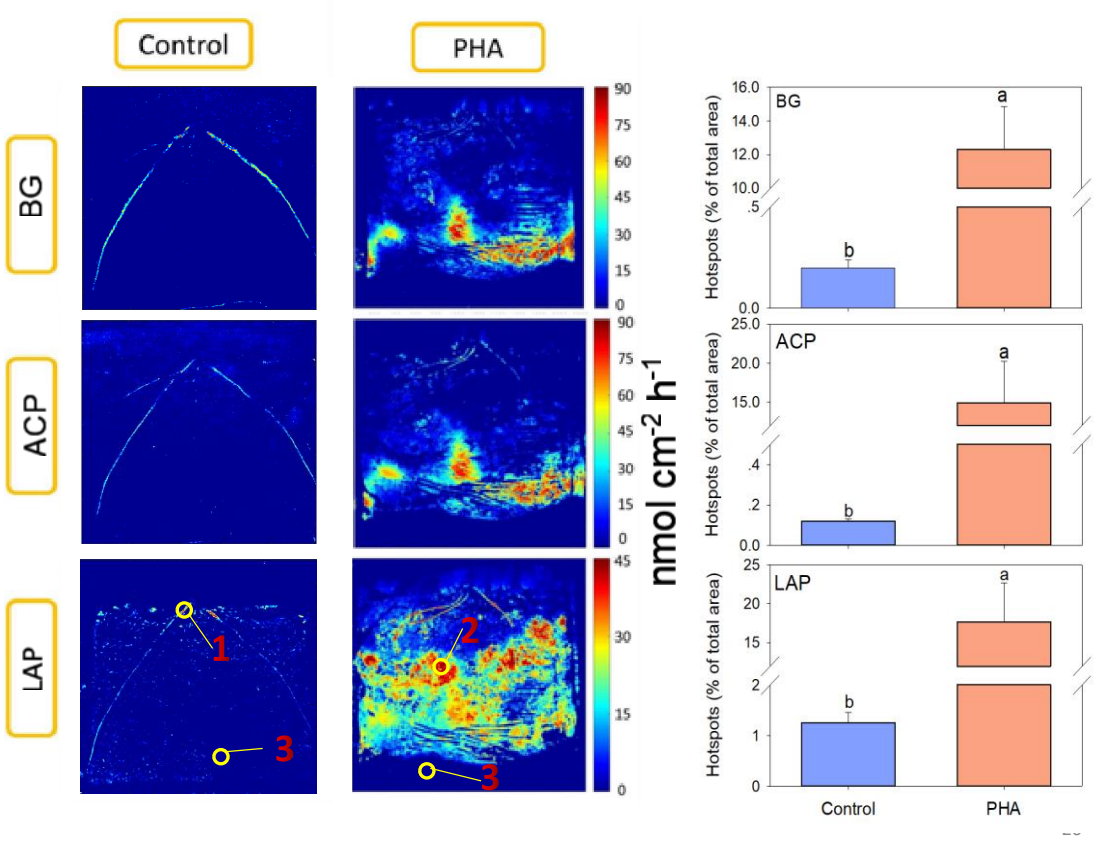

912

913 Fig. 2

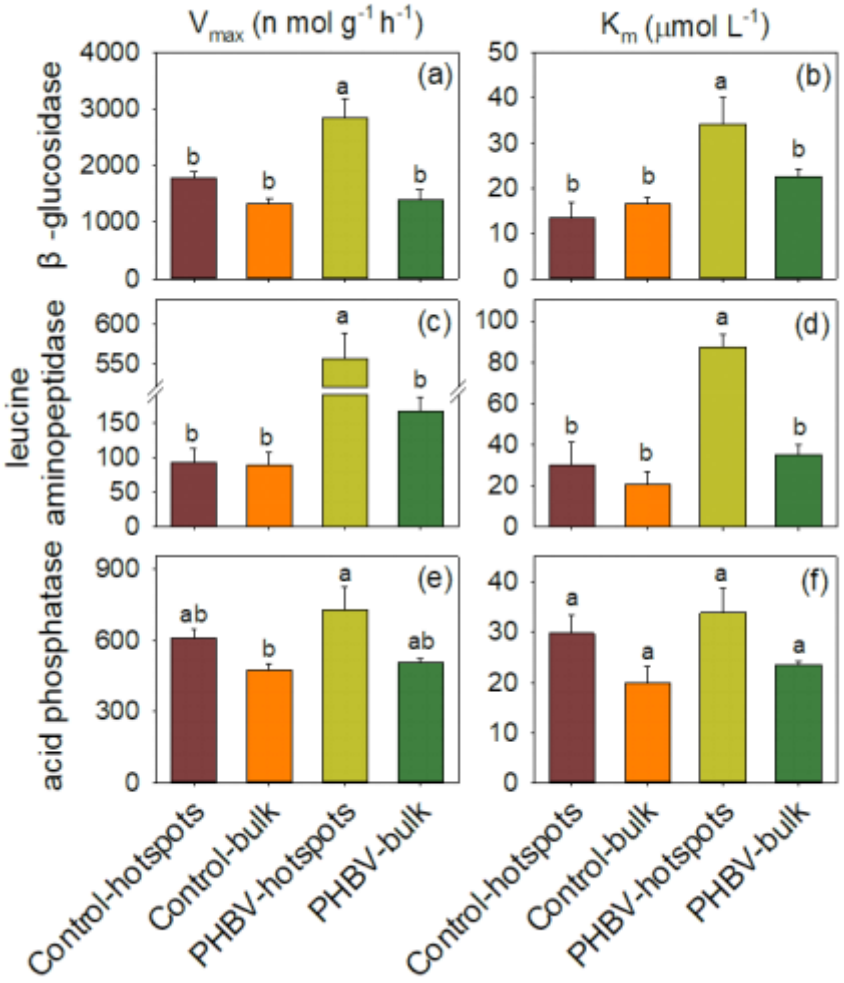
V_{max} (n mol g^{-1} h^{-1})
K_m (μmol L^{-1})
β -glucosidase
leucine aminopeptidase
acid phosphatase
(a)
(b)
(c)
(d)
(e)
(f)
Control-hotspots
Control-bulk
PHBV-hotspots
PHBV-bulk

914

915 Fig. 3

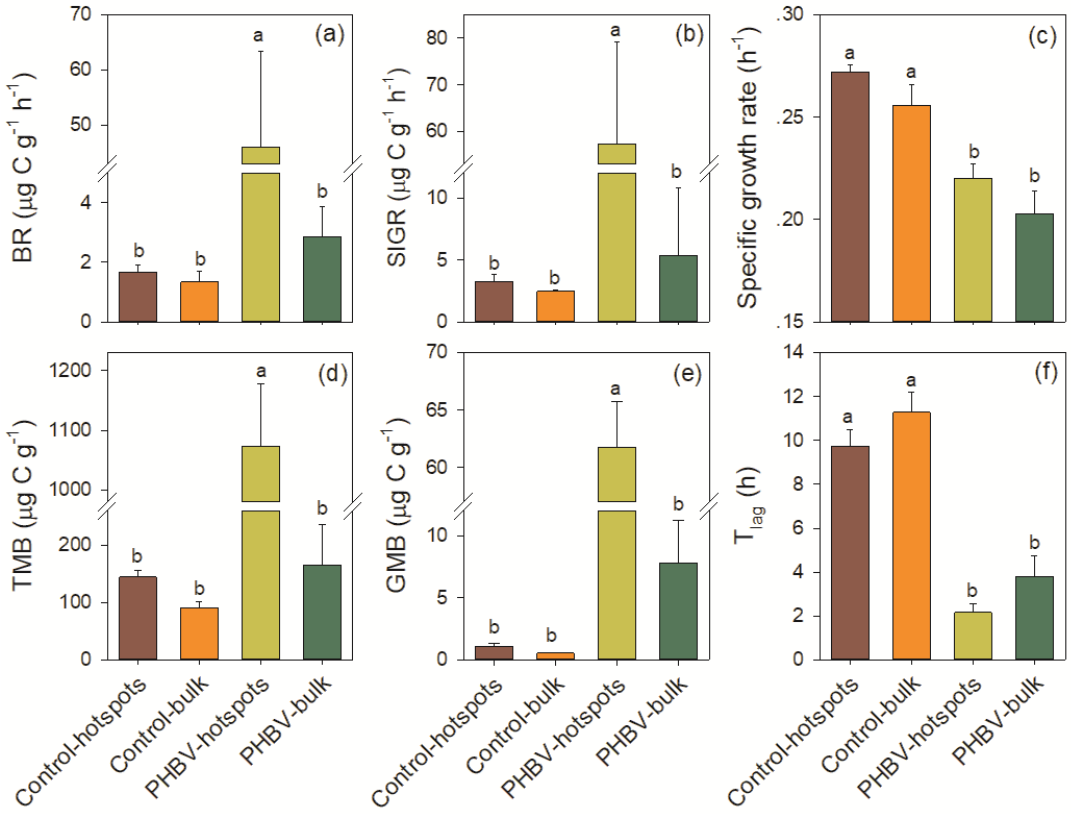

916

917

918

919 Fig. 4

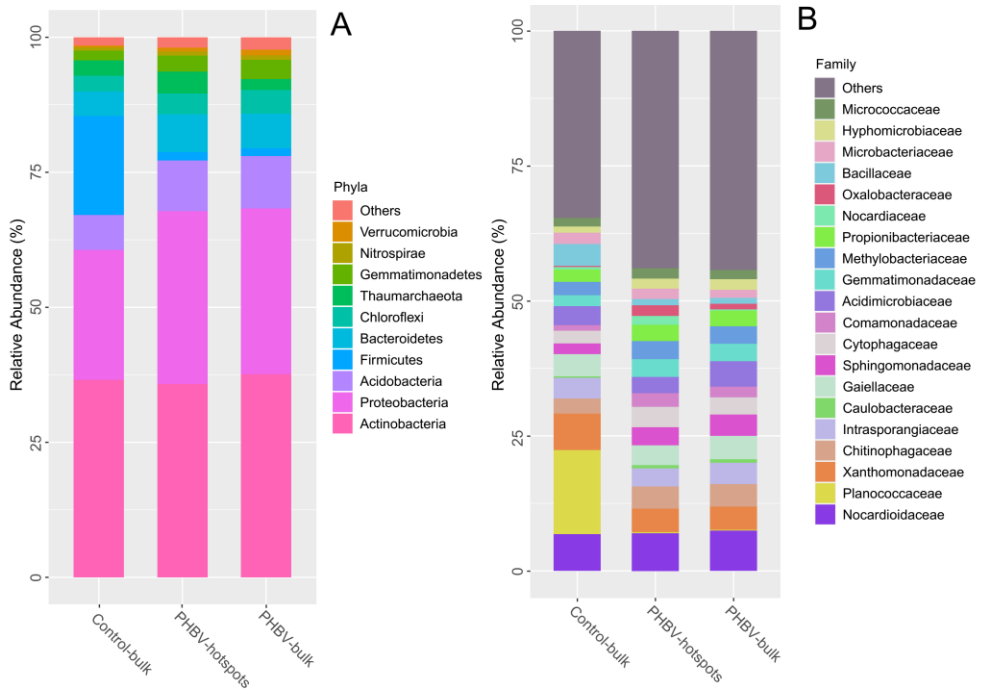
A
Relative Abundance (%)
0
25
50
75
100
Control-bulk
PHBV-hotspots
PHBV-bulk
Phyla
Others
Verrucomicrobia
Nitrospirae
Gemmatimonadetes
Thaumarchaeota
Chloroflexi
Bacteroidetes
Firmicutes
Acidobacteria
Proteobacteria
Actinobacteria
B
Relative Abundance (%)
0
25
50
75
100
Control-bulk
PHBV-hotspots
PHBV-bulk
Family
Others
Micrococcaceae
Hyphomicrobiaceae
Microbacteriaceae
Bacillaceae
Oxalobacteraceae
Nocardiaceae
Propionibacteriaceae
Methylobacteriaceae
Gemmatimonadaceae
Acidimicrobiaceae
Comamonadaceae
Cytophagaceae
Sphingomonadaceae
Gaiellaceae
Caulobacteraceae
Intrasporangiaceae
Chitinophagaceae
Xanthomonadaceae
Planococcaceae
Nocardioidaceae

920

921 Fig. 5

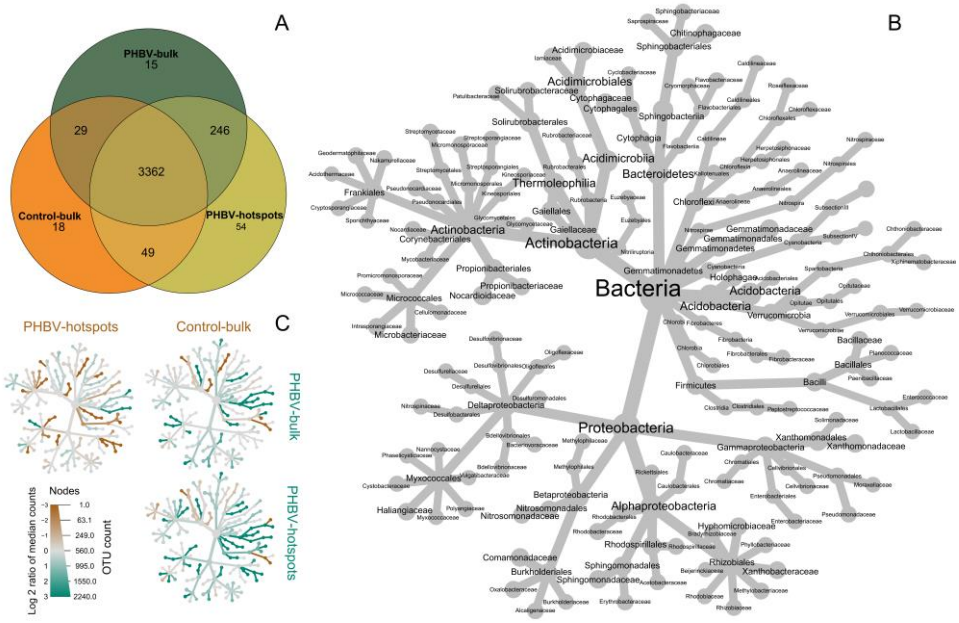

922

923

924 Fig. 6

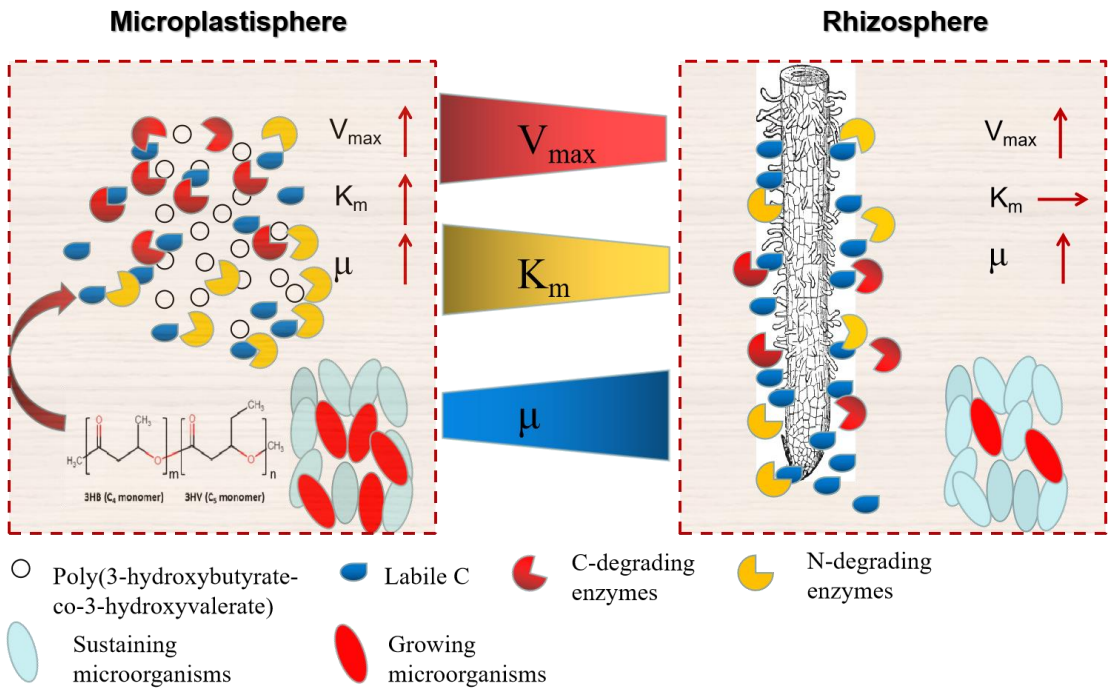

925

926